

Effect of Stator Resistance and Nonlinear Inductance on Field Weakening Operation of a Non-Salient Pole PMSM

Dr.-Ing. Radoslaw Nalepa, Andreas Noll, Moog GmbH
Dr.-Ing. Stephan Beineke, Dr.-Ing. Alexander Bähr, LTi DRIVES GmbH

Einfluss von Ständerwiderstand und nichtlinearer Induktivität auf den Feldschwächbetrieb von PMSM ohne ausgeprägte Schenklichkeit

Diese Publikation beschreibt Verbesserungen der Feldschwächfunktion von PMSM mit Oberflächenmagneten. Die Realisierung dieser Funktion wurde bereits in verschiedenen Publikationen beschrieben, allerdings ohne die Effekte der magnetischen Sättigung oder des Statorwiderstandes zu berücksichtigen.

Der vorliegende Artikel diskutiert eine effiziente und umsetzbare Lösung einschließlich der Programmfolge sowie eine Analyse bei variablen Motorparametern. Die Verbesserung wurde mit Hilfe einer Simulation nachgewiesen. Anschließend erfolgte eine Realisierung in einem High Performance Servoumrichter.

Keywords: field weakening, magnetic saturation, stator resistance

1. Introduction

High performance drives with high current density permanent magnets synchronous motors (PMSM) are frequently used in more and more demanding industrial applications. Numerous research works in this domain contributed to present level of digital control algorithms solutions and pulse width modulation (PWM) techniques [1], [4] as well as implementations of control and power electronics hardware [2], [3]. Nevertheless, there is still a place for improvements, perhaps not considered today as the basic ones but more likely application specific adjustments or market driven needs. Just few to mention: power electronics integration combined with efficient thermal management, reliable auto-tuning, active EMI control, safety functions implementation, robust systems communication, etc. Such demands may be satisfied once proven and reliable solutions are available in given area. All this is based on assumption that basic needs (e.g.: current control solutions or feedback signals processing) are already well enough satisfied.

This paper concentrates on one of the basic functionalities which in some circumstances may be considered as not well recognized and documented in a systematic way. Namely field weakening of PMSM with surface mounted rotor magnets. Such functionality extends effective constant power region of the torque-speed motor characteristic. Efficient and proven engineering solution is presented and discussed in this article including analysis of variation of selected motor parameters under magnetic saturation. A general recommendation for a program sequence is given. The solution has been verified in conjunction with a digital field oriented vector control scheme, Fig.1. Mathematical simulations have been conducted prior to real time implementation in a high performance drive.

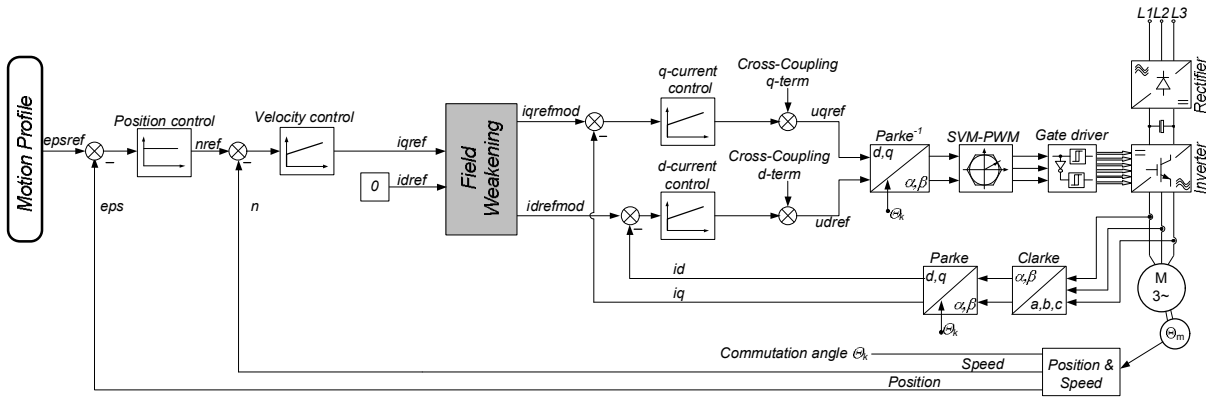


Fig 1. – General block diagram of field oriented vector control for a PMSM.

There is a number of publications, just few to mention [5][6][7], which treat the topic in a generic way with assumptions that the stator resistance of the motor equals to zero and magnetic saturation is not present. In addition they concentrate mainly on salient pole machines where the motor synchronous quadrature axis reactance, X_q , is significantly bigger than the direct axis, X_d . This in the end contributes to lack of reliable and simple engineering answer to field weakening if X_q is almost equal to X_d . Number of solutions with the assumption mentioned above have been tested with high performance magnetically saturated non-salient pole PMSM driven by high performance digital drives. In the end the stator resistance and magnetic saturation have proven to be rather significant in practice. Only one publication has been found recently, [8] – March 2008, addressing this issue taking in to account resistance and magnetic saturation, but again this in case of an interior permanent magnet machine and in rather scientific format. Therefore the issue was still remaining open at the time of writing this article. Demanding applications with non-salient poles PMSM, where enhanced performance in the constant power region contributes to higher process dynamics, were calling for an answer. At that stage our solutions had been already proven in several machines.

2. PMSM model and magnetic saturation

Well known steady-state equations of a PMSM can be written as following:

$$\begin{aligned} v_d &= R_s i_d - X_q i_q \\ v_q &= R_s i_q + X_d i_d + E \end{aligned} \quad (1)$$

where v_d and v_q are the d - and q -axis stator voltages, i_d and i_q are the d - and q - stator currents, R_s is the stator resistance, E is the back-EMF. The back-EMF can be expressed as:

$$E = \omega_e \psi \quad (2)$$

where ψ is the flux-linkage and ω_e is the electrical angular velocity. The synchronous reactances can be expressed as following:

$$\begin{aligned} X_d &= \omega_e L_d(i_d) \\ X_q &= \omega_e L_q(i_q) \end{aligned} \quad (3)$$

where L_d and L_q are the d - and q -axis inductances. The inductances are dependent of current. Here, for a simplicity reason, we neglect the split of synchronous reactance to the main one and the leakage one.

In case of a PMSM with surface mounted rotor magnets the direct and the quadrature axis inductances are almost equal. This is true when operating point is not in magnetic saturation region, Fig.2. In such a condition L_q of Moog's motors is slightly bigger than L_d , normally less than a few percent.

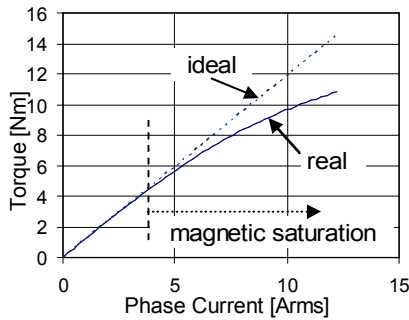


Fig. 2: Torque-Current characteristic of Moog PMSM (G463L25).

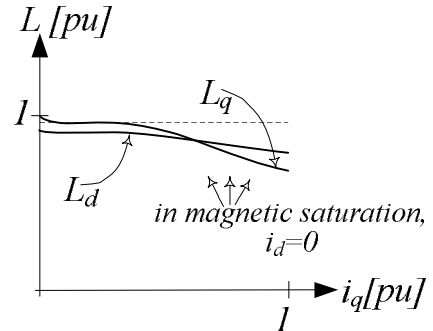


Fig. 3: Inductance variation with i_q change.

In magnetic saturation region, when larger currents flow in windings of the stator, L_q and L_d become smaller than their initial values, Fig.3. Drop of L_q is normally bigger than L_d - this is in case of operation without field weakening, $i_d=0$. Rough information about L_q variation in function of i_q current can be extracted from motor torque vs. current characteristic which normally should be a part of the motor data sheet, Fig.2. In case of operation with field weakening, $i_d < 0$, situation is different. The L_d stays more or less constant or can even slightly increase, Fig.5. This is due to the demagnetization effect, Fig.4b, as the direct axis current is decreasing and acting opposite the flux. The L_q drop can be slightly smaller when compared to operation with $i_d=0$. Overall inductance variation of a PMSM has been investigated in details based on its decoupled (in terms of current) measurements, Fig.6. Additional motor parameters variations due to the tolerance or thermal effects, for simplicity reasons, are not discussed in this article. In the reality that must be taken into account, [9], during overall drive stability analysis.

Torque produced by a PMSM can be described according to the following equation:

$$T = \frac{3}{4} p [(L_d - L_q) i_d i_q] + k_t i_q \quad (4)$$

where p is number of PMSM poles and k_t is the motor torque constant. At this point it is worth to mention that the torque equation commonly used in its simplified form, when L_d is assumed to be equal to L_q , is somehow misleading – especially in case of high power density PMSM, when operation in magnetic saturation is allowed.

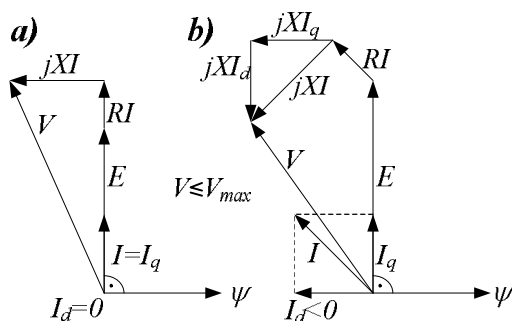


Fig. 4: Phasor diagram of non-salient pole sine wave PMSM. (a) standard motoring mode, (b) demagnetizing effect with field weakening.

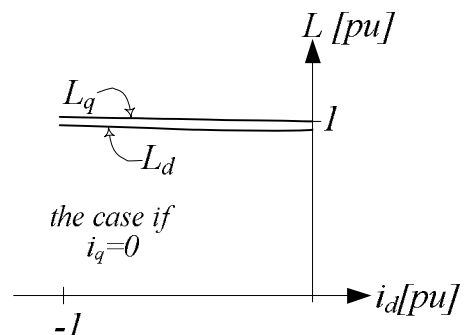


Fig. 5: Inductance variation with i_d change.

For completeness it must be mentioned that there are two constrains in physically running PMSM, [1]. The first one is related to the thermal limits of the motor and it is expressed as following:

$$i_d^2 + i_q^2 \leq i_{\max}^2 \quad (5)$$

where i_{\max} is the maximum allowed motor current in [A_{pk}]. The second one is related to the voltage limit:

$$v_d^2 + v_q^2 \leq v_{\max}^2 \quad (6)$$

where v_{\max} is the maximum available voltage at the motor terminals. Generally it can be expressed as a function of the DC-bus voltage, $v_{\max} = V_{dc}/\sqrt{3}$.

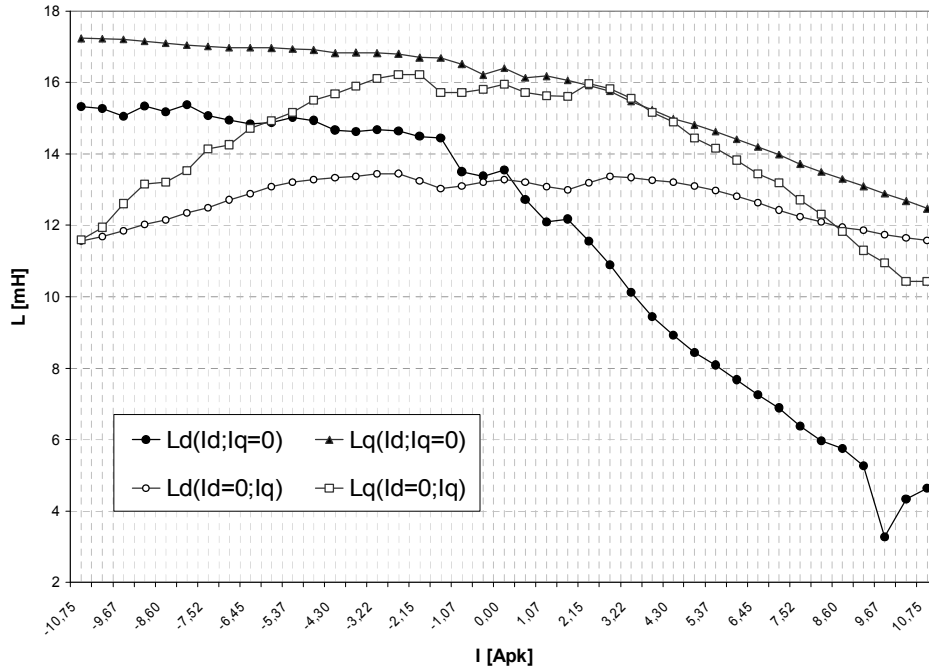


Fig. 6: L_d and L_q inductances of Moog PMSM (G463L25) in function if i_d and i_q currents.

3. Field Weakening Equations

Natural constrains expressed by equation (5) and (6) combined with equations (1)-(3) lead to theory of field weakening [1]. According to the theory creation of higher torque at higher motor speed is possible when combined with the control scheme shown in Fig.1. It is achieved by maintaining higher i_q and also utilizing, to a certain extent, “ $(L_d - L_q)$ ” part of equation (4) in the constant power region. In other words, instead of keeping the $i_d=0$ and naturally limiting i_q (standing in this case for peak motor phase current), Fig.7a, both i_d and i_q are manipulated in such a way that resultant motor phase current is larger and at the same time does not exceed the maximum allowed trajectory, Fig.7b. The maximum trajectory is set by intersection point between current limit circle and voltage limit circle.

The current limit is normally fixed for a motor unless it is reduced by a thermal limiting mechanism. The voltage limit varies with electrical frequency and values of resistance, inductance and the back EMF according to the following equation:

$$\left(i_d + \frac{XE}{Z^2} \right)^2 + \left(i_q + \frac{R_s E}{Z^2} \right)^2 = \left(\frac{v_{\max}}{Z} \right)^2 \quad (7)$$

which is a result of substitution of (1) and (2) into (6) with assumption that $X_d=X_q=X$ and $Z^2=R_s^2+X^2$. It is worth to notice that (7) complies with well known equation of a circle in xy coordinates with a radius of r :

$$(x - x_0)^2 + (y - y_0)^2 = r^2 \quad (8)$$

Based on (7), it can be seen that minimum sensible direct-axis current is as following:

$$i_{d \min} = -\frac{XE}{Z^2} \quad (9)$$

Further continuing along the maximum current locus, below the $i_{d \min}$, will contribute mainly to heat generation in the motor. Second coefficient of the centre point of the voltage limit circle is:

$$i_{q \text{ shift}} = -\frac{R_s E}{Z^2} \quad (10)$$

It can be seen that it shifts the centre point (or in other words reduces allowed i_q). This information is lost if the stator resistance, R_s , is assumed to be equal to zero. Notice that (10) changes sign together with the velocity.

Substituting (5) into (7) with assumption that the $i_d=0$ and solving for i_q allows to find maximum allowed q -axis current, $i_{q \max}$, at a given voltage limit:

$$i_{q \max} = \frac{-R_s E + \sqrt{v_{\max}^2 Z^2 - X^2 E^2}}{Z^2} \quad (11)$$

With equation (11) a criteria for activation of the field weakening algorithm can be set. It could look e.g.:

if q -axis current command $\leq i_{q \max}$
then
 pass through the q -axis current command;
 keep the d -axis current equal 0;
else
 ...start modifying the d - and q - currents (activate field weakening)

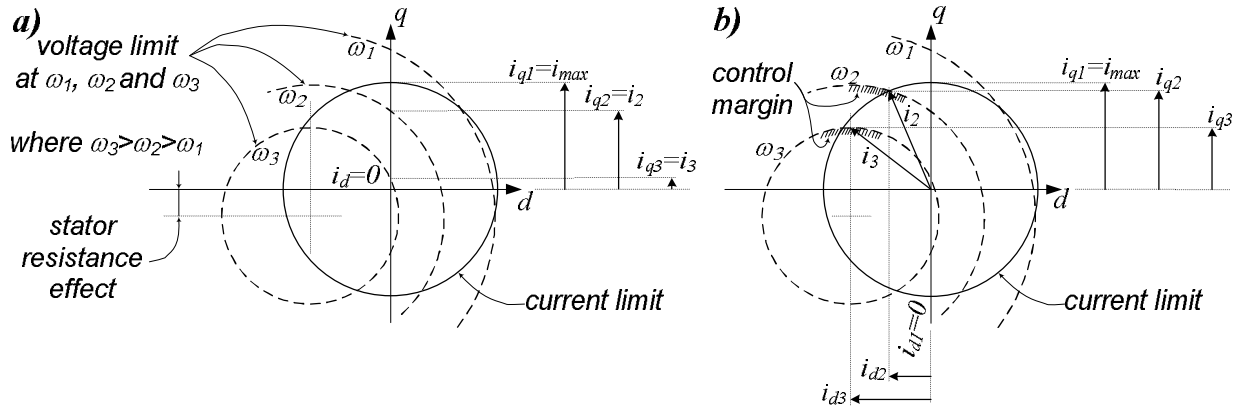


Fig. 7: Current/voltage limit circles versus field weakening a) disabled, b) enabled.

Once the operating point is in the area where field weakening is needed a few more equations is needed. The d - and q - currents at the intersection point, $i_{d \text{ int}}$ and $i_{q \text{ int}}$, of the voltage and the current circles can be expressed as following:

$$i_{d \text{ int}} = -\frac{1}{2} \frac{XZ^2(i_{\max}^2 Z^2 + E^2 - v_{\max}^2) + \sqrt{Z^4(X^2 - Z^2)((v_{\max}^2 - E^2)^2 + Z^2 i_{\max}^2 (Z^2 i_{\max}^2 - 2E^2 - 2v_{\max}^2))}}{Z^4 E}$$

$$i_{q \text{ int}} = \sqrt{(i_{\max}^2 - i_{d \text{ int}}^2)} \quad (12)$$

It is derived from substitution of (5) into (7) with assumption that the d -axis current is not equal to zero, $i_d \neq 0$. If the q -axis current command (i_{qcmd}) is less than i_{qint} then $i_{drefmod}$ can be calculated from (7) with assumption that $i_q = i_{qcmd}$:

$$i_{drefmod} = \frac{-XE + \sqrt{X^2E^2 - Z^2(i_{qcmd}^2 Z^2 + 2i_{qcmd}^2 R_s E + E^2 - v_{max}^2)}}{Z^2} \quad (13)$$

Using equations (9) to (13) a complete field weakening algorithm for PMSM can be developed. The equations have been used as foundation to derive auto calculation criteria for field a weakening method based on a lookup table, which is discussed later in this article.

4. Field Weakening Implementation

A number of methods have been analysed before the final implementation. Three of them have proven to be particularly good and they will be presented in more details:

- 1st - a voltage follower based on a PI voltage compensator adjusting the d - current while the q - current is left to its natural limitation, Fig.8a.
- 2nd - automatically set 3D look-up table where the d - current is given in function of speed, the q - current and the DC bus voltage. The q - current is left to its natural limitation, Fig.8b.
- 3rd - a solution based on combination of the 1st and the 2nd method, Fig.9.

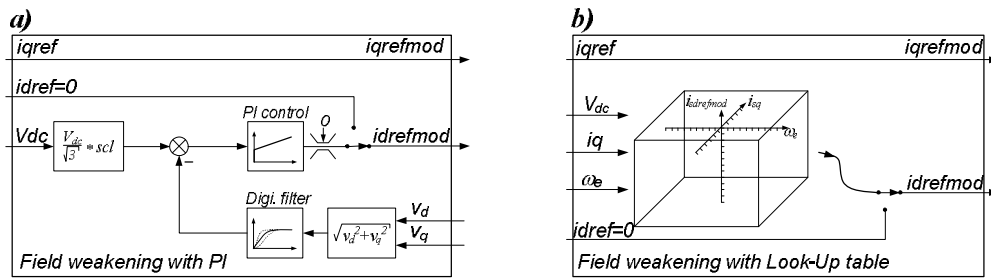


Fig. 8: Simplified block diagram of field weakening scheme based on: a) PI voltage compensator, b) 3D look-up table.

4.1 Field Weakening with a PI Voltage Compensator

The voltage compensator is shown in Fig.8a. The reference motor voltage is a fraction 80..100% of the maximum available voltage v_{max} , "scl" in Fig.8a and Fig.9. The actual voltage value is computed from the two current controller outputs. The voltage is controlled by varying the d - reference current from zero down to a minimum value. Care must be taken that the minimum value is above the value from (9), otherwise the control may become instable. The method is not very sensitive to variation of the motor parameters.

This method has proven to be the most reliable among the three. Its tuning recommendations have been derived for PMSM. The control gains are calculated and set automatically in the drive software - based on the motor parameters. Major difficulty in this case is related to the best DC bus voltage utilization versus high and low dynamics of a driven system. In case of low dynamics motion the voltage margin can be small, say <5%, but in opposite case even 10% or more may be needed. In case of a process with wide range of changes of motion dynamics the bigger margin should be applied. The margin helps to deal with issues related to control on the limit. This issue is successfully treated with a feed-forward control solution discussed later.

4.2 Field Weakening with a Three-dimensional Look-up Table

Experiments with a manually set 2D look-up table and with a real time calculated equations (5) and (7) have led to a new solution. The assumption $R_s=0$ has proven to be unacceptable in case of many motors used in practice. The new solution is based on auto-calculated 3D look-up table where the d - current depends on ω_e , i_q and the DC bus voltage, Fig.8b. Values of the table are computed in the servo controller based on discussed earlier equations, ($R_s \neq 0$), and given motor parameters, Table 1. For each operating point (ω_e , i_q), the corresponding i_d is computed following proper checks against discussed earlier conditions. During real time run a linear interpolation is used between the pre-calculated operating points.

The DC bus voltage has been taken into account by using it in scaling of the speed input, " ω_e/V_{dc} ", this with assumption that the motor voltage scales almost proportional with the speed.

The advantage of this method is that relatively accurate field weakening current is available immediately, as opposed to the voltage compensator with a limited bandwidth. The word "relatively" is related to neglect for tolerance, thermal and magnetic saturation effects on motor parameters. Additional advantage is related to reduced real time processing when compared to online computing of a complete set of equations and conditions.

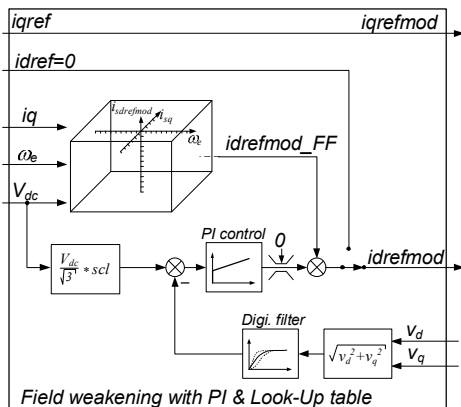


Fig. 9: Simplified block diagram of field weakening scheme based on PI compensator and a 3D look-up table.

Parameter Name	Value
Stator resistance, R_s	6.5Ω
d -axis inductance, L_d	13.22mH
q -axis inductance, L_q	14.15mH
EMK constant, k_e	0.97Vpk/rad/s
Rated current, I_n	1.9Arms
Peak stall current, I_{max}	8.0Arms
Rated torque, M_n	2.21Nm
Peak stall torque, M_{max}	8.3Nm
Rated speed, N_n	4800rpm
No load speed, N_0	5560rpm
Maximum speed, N_{max}	7880rpm

Table 1. Parameters of PMSM, type G463L25.

4.3 Field Weakening with a PI Voltage Compensator and a 3-D Look-Up Table

The PI and the 3D look-up table have been combined together in order to get the best out of the two methods. Such a scheme can be compared to a PI controller with a feed-forward path, Fig.9. The table is a source of immediate, relatively accurate, d - axis current set points and the PI compensator takes care of final adjustments. The q - current is naturally limited by the available motor voltage.

Such a scheme provides robust dynamic performance and properly deals with effects of motor parameters variations due to magnetic saturation, temperature rise and components tolerance.

5. Experimental results

During laboratory tests static and dynamic performance has been investigated in details for discussed field weakening methods. Static performance has been recorded in form of torque-speed characteristics and corresponding d - and q - axis currents. Dynamics has been analysed during rapid reverse operation with a tested motor without a load.

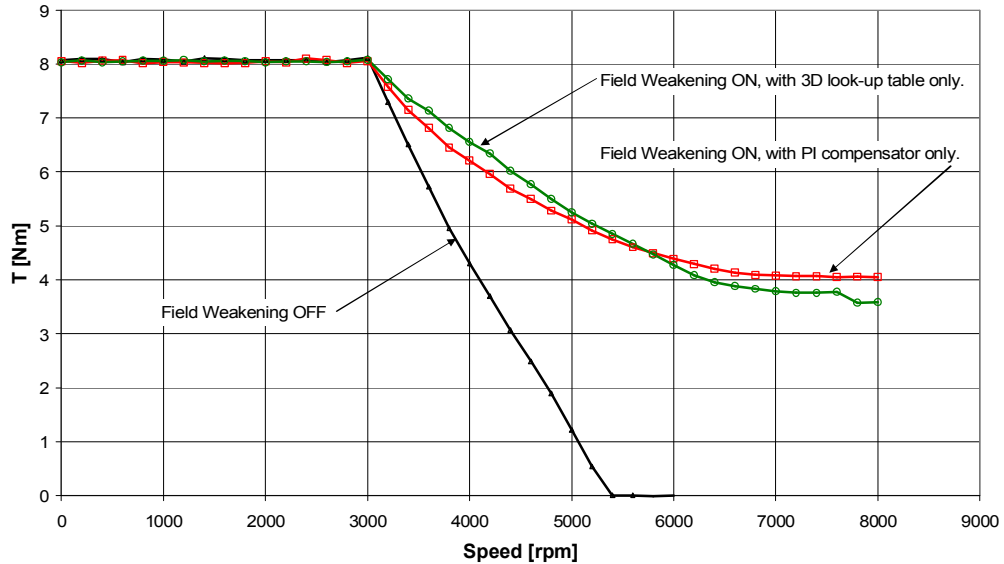


Fig. 10: Torque-speed plots for a PMSM with and without field weakening, Moog motor: G463L25.

It can be seen in Fig.10 that torque-speed characteristic is significantly higher in constant power region if field weakening is activated. The performance with 3D look-up table is similar to the PI compensator. This confirms rather optimal settings of the table values. Small advantage of the table over the PI scheme at lower speeds can be explained by the voltage control margin present in case of the PI, $scl=5\%$ in this case.

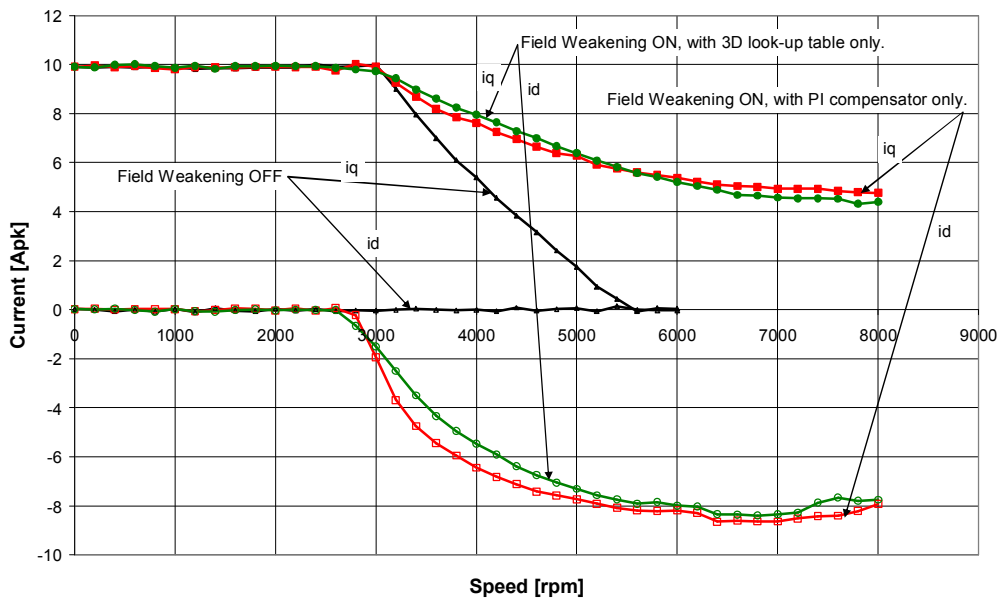


Fig. 11: Corresponding currents for torque-speed plots from Fig.10.

The PI compensator selects better current trajectory at higher speeds where the magnetic saturation still influences L_q , analyse Fig.6 in combination with Fig.2 and Fig.11.

Records of dynamic performance tests can be seen in Fig.12 and Fig.13. Tests have been performed for three scenarios described in §4.1, §4.2 and §4.3. The PI compensator on its own does not follow closely the reference speed near to the corner, Fig.12. In this case the voltage control margin was set to 10% and contributed to this error. It gets better with the 3D look-up table. Speed response is close to the reference with a small overshoot. This is achieved with noticeably faster and higher d -axis current response, Fig.13.

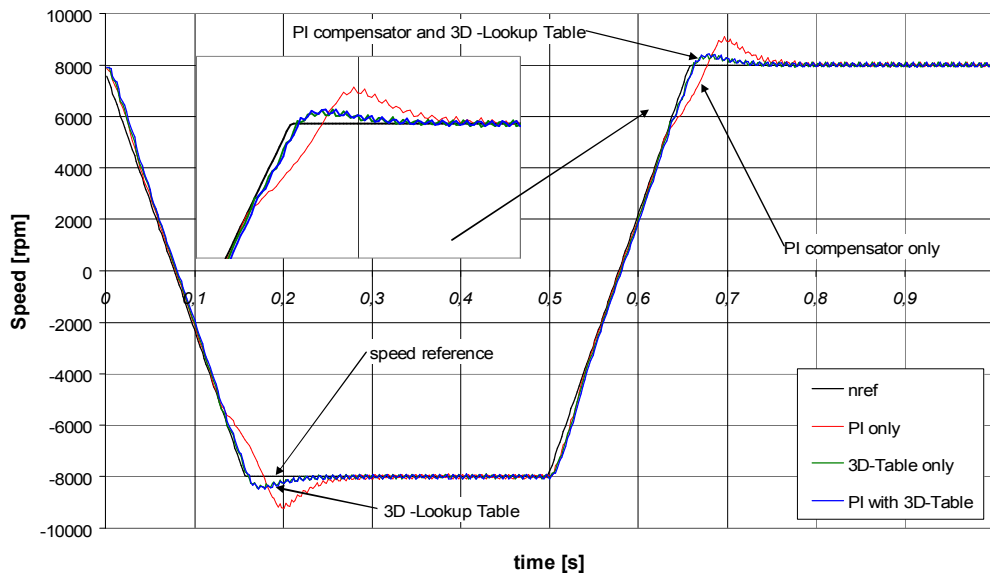


Fig. 12: Speed plots with field weakening for Moog motor: G463L25 – dynamic reverse mode.

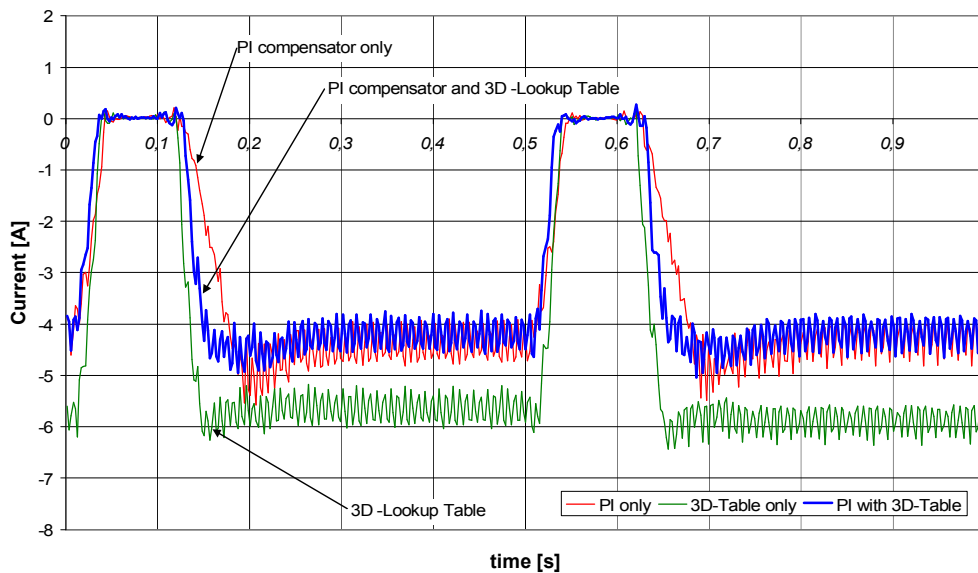


Fig. 13: Corresponding currents for speed plots from Fig.12.

Further dynamic performance improvement can be achieved when the table is combined with the PI compensator. In terms of speed response it is rather difficult to distinguish the difference when compared to the table on its own, Fig.12. An advantage is clear when currents from Fig.13 are analysed. Matching performance is achieved with slower and smaller in steady state d -axis current. It can be noticed that

the current changes faster than with the PI compensator but settles at the same level. This reduces the thermal heat in the motor without performance loss.

6. Summary

Reliable and proven engineering solutions for field weakening for a non-salient pole PMSM have been presented in this article. Discussed material leads to good understanding of fundamental issues related to this topic. The stator resistance and the motor inductance under magnetic saturation have been taken into account. Based on given equations and shared information different (from presented) practical field weakening solutions can be derived.

Presented solutions have been proven in real machines in plastics forming industry where rapid and precise movements are the key factors of an efficient process. Based on up to date experience - combination of a PI compensator and a look-up table as a feed forward seems to be the most optimal field weakening solution in presence of the motor parameters variations.

7. References

- [1] Edited by B.K. Bose: "Power Electronics and Variable Frequency Drives – Technology and Applications", *IEEE press*, 1997 New York.
- [2] N. Mohan, T.M. Undeland, W.P. Robbins: "Power Electronics – Converters, Applications and Design", *John Wiley & Sons, Inc.*, 1995 New York.
- [3] C. Winterhalter, R. Kerkman, D.W. Shlegel, D. Leggate: "The effect of Circuit Parasitic Impedance on the Performance of IGBTs in Voltage Source Inverters", *IEEE Applied Power Electronics Conference (APEC'01)*, 4-8 March 2001, Anaheim, California, US.
- [4] J.O. Krah, J. Holtz: "High-Performance Current Regulation and Efficient PWM Implementation for Low-Inductance Servo Motors", *IEEE Transactions on Industry Applications*, vol.35, No.5, Sep/Oct 1999.
- [5] A.K. Adnanes, T.M. Undeland: "Optimum Torque Performance in PMSM Drives Above Rated Speed", *IEEE IAS Annual Meeting Rec.*, 1991.
- [6] W.L. Soong, T.J. Miller: "Theoretical Limitations to the Field-Weakening Performance of the Five Classes of Brushless Synchronous AC Motor Drive", *6th international Conference on Electrical Machines and Drives*, 8-10 Sep. 1993.
- [7] S.M. Sue, C.T. Pan "Voltage-Constraint-Tracking-Based Field-Weakening Control of IPM Synchronous Motor Drives", *IEEE Transactions on Industrial Electronics*, Vol.55, No.1, January 2008.
- [8] C. Jo, J.Y. Seol, I.J. Ha: "Flux-Weakening Control of IPM Motors with Significant Effect of Magnetic Saturation and Stator Resistance", *IEEE Transactions on Industrial Electronics*, Vol.55, No.3, March 2008.
- [9] J.F. Moynihan: "Aspects of Digital Current Control for AC Drives", *Elaborate by PEI Technologies, Ireland*, 1996.